Element-Specific Probe of the Magnetic and Electronic Properties of Dy *incar*-Fullerenes

F. Bondino,*,† C. Cepek,† N. Tagmatarchis,‡,§ M. Prato,§ H. Shinohara,⊥ and A. Goldoni||

Laboratorio Nazionale TASC, INFM-CNR, S.S. 14 km 163.5 in Area Science Park, 34012 Trieste, Italy, Theoretical and Physical Chemistry Institute, National Hellenic Research Foundation, Vass. Constantinou 48 Avenue, 116 35 Athens, Greece, Dipartimento di Scienze Farmaceutica, Università di Trieste, Piazzale Europa 1, 34127 Trieste, Italy, Department of Chemistry, University of Nagoya, 464 8602 Nagoya, Japan, and Sincrotrone Trieste S.C.p.A., S.S. 14 Km 163.5 in Area Science Park, 34012 Trieste, Italy

Received: October 17, 2005; In Final Form: February 15, 2006

The magnetic and electronic properties of a single atom and a pair of Dy atoms encapsulated inside fullerene carbon cages have been examined using X-ray absorption spectroscopy (XAS) and X-ray magnetic circular dichroism (XMCD) as well as resonant photoelectron spectroscopy (RESPES) across the Dy $M_{4,5}$-edge. The comparison of the measured XAS spectra with multiplet calculations indicates that the encaged Dy has a $4f^9$ configuration. The presence of Dy 5d spectral weight in the valence band is not detected by RESPES, indicating that Dy is in a formally trivalent state. The evolution of the encaged Dy orbital and spin moments of the 4f orbitals as a function of the applied magnetic field and temperature has been obtained from XMCD measurements. At 6.9 T and 4 K, both the orbital and the spin magnetic moments of the encaged Dy 4f electrons are dramatically smaller than those expected for the free Dy^{3+} at saturation.

I. Introduction

incar-Fullerenes, known also as endohedral fullerenes, are a novel kind of molecular compounds, consisting of metal atoms, clusters, or carbides encapsulated in the inner empty space of a carbon cage.[1] The unique structure of these materials and the possibility to control the properties by changing the size of the cage and the number, nature, and kind of the encaged atoms is expected to lead to new materials with remarkable physical properties and potential applications. For instance, atoms with high magnetic moments, such as Gd, Dy, and Ho, encapsulated in fullerenes or fullerenols, $C_{60}(OH)_n$, are materials with potential use as magnetic resonance imaging (MRI) contrast agents,[2−6] diagnostic and therapeutic radiopharmaceuticals,[7] photoelectrochemical cells,[8] and molecular memories.[9]

Despite the large number of investigations of these systems, the magnetic properties of the core atoms and the extent of the interaction between the core atom and the carbon cage are still open points. The charge transfer between the core atom and the carbon cage is an important quantity, and several studies have been performed to establish the effective valence of the encaged ion. In several cases, a purely ionic picture was not sufficient to describe the electronic structure of *incar*-fullerenes. For example, the core ions of $La@C_{82}$ and $Sc@C_{84}$, originally thought to be purely trivalent and divalent ions, respectively, were found to be more correctly described by the inclusion of a finite hybridization between the core atom and the fullerene cage.[10,11]

The effective valence state of the core atom and the metal−cage interaction play an important role in the magnetic properties of the *incar*-fullerenes. In $Ho@C_{82}$ a dramatic reduction by 40% of the magnetic moment with respect to free Ho^{3+} was observed. This behavior was ascribed to the carbon cage crystal field effect and to the partial hybridization between the metal and the carbon cage orbitals.[12] Differently, in $Gd@C_{82}$ the magnetic moment of the system is close to that of the free Gd^{3+} ion, and photoemission measurements indicate a complete charge transfer from Gd to the C_{82} cage.[13] In $La@C_{82}$, superconducting quantum interference device (SQUID) measurements found an average magnetic moment larger than the one expected for free La^{3+} ion[14] probably due to the incomplete charge transfer.[10]

For $Dy@C_{82}$, Mössbauer measurements find paramagnetic relaxation at 4.2 K and an isomer shift consistent with the Dy^{3+} state and a full charge transfer to the fullerene cage.[15]

Magnetic susceptibility measurements[12] indicate a paramagnetic relaxation even at 1.8 K with the $Dy@C_{82}$ system having a magnetic moment reduced by 13−20% with respect to the full moment value of trivalent Dy. It is also interesting to investigate the valence state of the encaged Dy atom since a valence change from the trivalent to the lower valence state is expected to occur when the coordination number is reduced to less than 4 atoms.[16,17] Previous studies using the Dy L_3-edge X-ray absorption spectroscopy (XAS) of $Dy@C_{82}$ indicate a Dy^{3+} charge state.[18] Furthermore a variation of the valence state from Dy^{3+} to Dy^{2+} was found by potassium intercalation into the $Dy@C_{82}$ crystals.[19] However, recent calculations indicate the existence of cage−metal hybrid states[20] in contrast to a purely ionic picture of this system. Very recently, an investigation of different lanthanide *incar*-fullerenes using X-ray magnetic circular dichroism (XMCD) has been reported.[21]

Here we report on XAS, XMCD, and resonant photoelectron spectroscopy (RESPES) measurements performed at the Dy $M_{4,5}$-edge of a $Dy@C_{82}$ mono-*incar*-fullerene and two different $Dy_2@C_{88}$ di-*incar*-fullerene isomers in the temperature range of 4−300 K under applied magnetic fields from 0 to 6.9 T.

* Author to whom correspondence should be addressed. E-mail: bondino@tasc.infm.it.
† Laboratorio Nazionale TASC.
‡ National Hellenic Research Foundation.
§ Università di Trieste.
⊥ University of Nagoya.
|| Sincrotrone Trieste S.C.p.A.

10.1021/jp055938z CCC: $33.50
Published on Web 03/22/2006

These measurements aim at establishing the element-specific electronic and magnetic properties of these compounds, taking advantage of the elemental and orbital sensitivity of X-ray core-level spectroscopies at resonance conditions. The study of the magnetic properties exploits the capability of XMCD to provide orbital-selective signals localized on a specific ion. From the experiment, we examine the valence state of the metal, the orbital hybridization and electronic charge transfer between the metal and the carbon cage, the effective magnetic moment of the Dy ion inside the carbon cage, and the dependence of the orbital magnetic moment on isomer symmetry, temperature, and number of encapsulated atoms. X-ray absorption spectroscopy measurements in conjunction with multiplet calculations can give quantitative information on the 4f electron occupancy in the ground state. From RESPES, the extent of charge transfer from Dy to the carbon cage and, in particular, the presence of Dy 5d states in the valence band are investigated.

II. Experimental Section

The experiments were performed at the BACH beamline of ELETTRA.[22] Linearly and circularly polarized light in the 35−1600 eV range is provided by two APPLE II helical undulators. The circular polarization rate over the full Dy $M_{4,5}$-edge was 81% using the fifth harmonic. The resolving power of the monochromator was set to 1800 in the Dy $M_{4,5}$-edge photon energy.

Soot containing various Dy metallofullerenes was produced by the direct current arc discharge method of Dy_2O_3/graphite composite rods (12.5 mm × 12.5 mm × 300 mm, 0.8 wt %, Toyo Tanso Co.).[23,24] The dysprosium composite rods were heat-treated at a high temperature of 1600 °C. These rod conditions have been found to be crucial for the efficient production of this kind of metallofullerenes via the arc discharge method. The so-produced soot was collected under totally anaerobic conditions to avoid any degradation from air during the collection procedure. Then, it was Soxhlet-extracted first by carbon disulfide and then by pyridine. High-performance liquid chromatography (HPLC, LC-908-C60, Japan Analytical Industry) was performed for the separation of dysprosium endohedrals using Buckyprep (20 mm × 250 mm, Nakalai Tesque), 5PYE (20 mm × 250 mm, Nakalai Tesque), and Buckyclutcher (20 mm × 300 mm, Regis Chemical) columns. The purity of the newly synthesized materials (>99%) was confirmed by both positive and negative laser-desorption time-of-flight (LD-TOF) mass spectrometry. A few droplets of *incar*-fullerene solution were deposited on an Au substrate and then inserted inside the ultra high vacuum (UHV) chamber (10^{-10} mbar). A brief annealing in UHV at ∼350−400 K was carried out before the acquisition of the spectra to remove the solvent CS_2.

The XAS and XMCD measurements were carried out in a UHV 4 K cryostat hosting a superconducting magnet able to deliver magnetic fields from 0 to 7 T.[25] The absorption spectra were recorded in total electron yield, collecting simultaneously the photocurrent emitted by the sample and the reference current I_0 from the last refocusing mirror of the beamline. The XAS data have been normalized by I_0 to the absorption edge jump and background-subtracted.

The XMCD measurements were performed with the sample in a magnetic field applied perpendicularly to the sample surface and along the light propagation direction. At each temperature and at each applied magnetic field two pairs of spectra were obtained by reversing the direction of the magnetic field and the light helicity. The XMCD signal calculated as the difference between the spectra obtained by flipping the direction of the magnetic field or the helicity of the light was practically the same. The comparison of the XMCD signal obtained in these two ways provides a method to monitor the reliability of the results especially in the case of weak dichroism signals.

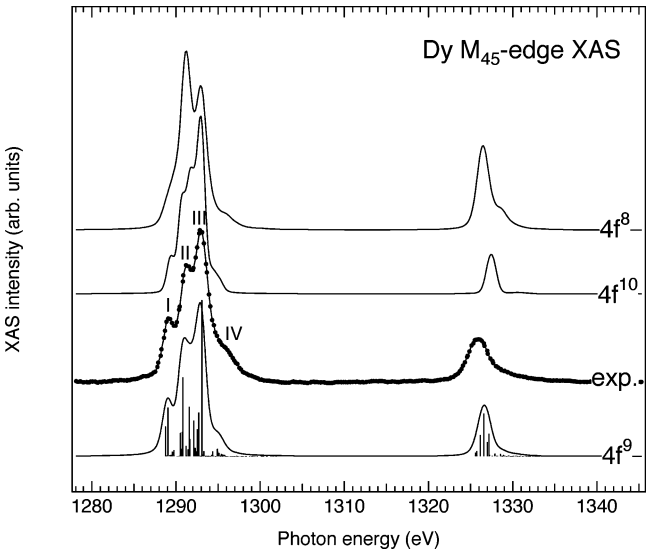

Figure 1. Dy $M_{4,5}$-edge XAS experimental spectrum of the $Dy_2@C_{88}$ isomer II measured at 300 K without magnetic field after background subtraction and the results of atomic calculations performed for different ground-state configurations.

The RESPES measurements were performed using a modified 150 mm VSW hemispherical electron analyzer with a 16-channel detector. The RESPES measurements were performed at normal incidence of the photon beam. Each photoemission spectrum was fitted with a sum of a cubic polynomial background and five Voigt functions.

III. Results

A. X-ray Absorption Spectroscopy. Figure 1 shows the Dy $M_{4,5}$-edge isotropic XAS spectrum of the $Dy_2@C_{88}$ isomer II. The spectrum consists of two well-separated line groups due to the strong spin−orbit interaction. These lines can be described as final-state multiplet structures arising from the strong intermediate coupling due to the electrostatic interactions between 4f electrons and between the 3d hole and the localized 4f electrons. To determine the number of unoccupied 4f electrons in Dy, the $M_{4,5}$-edge XAS spectra have been calculated for $4f,^9$ $4f,^{10}$ and $4f^8$ ground-state configurations to $4f^{n+1}$ final states ($n = 10, 11, 12$, respectively). The calculations have been performed using Cowan's code within the multiplet formalism on the basis of the relativistic Hartree−Fock (HF) approximation with a semiempirical reduction of the Slater integrals from the atomic results.[26,27] The Slater integrals of electrons within the same shell F^k(ff) have been scaled down by 60%, while the Coulomb and exchange integrals of electrons within different shells, F^k(df) and G^k(df), have been scaled by 70% of the HF values. The multiplet lines have been further rescaled for a Boltzmann distribution, and a rigid shift of the energy scale has been applied to match the experimental spectra that have been calibrated with the photoemission measurements. The final spectrum is obtained by convolution of the multiplet lines with a Gaussian broadening ($\sigma = 0.4$ eV) and a Lorenzian broadening ($\Gamma = 0.3$ eV).

In Figure 1 the results of the multiplet calculations performed for different ground-state configurations are compared with the experimental Dy $M_{4,5}$-edge XAS spectrum of $Dy@C_{82}$. The experimental spectrum appears to be well consistent with a $4f^9$

ground-state configuration with a good correspondence both in the position and in the branching ratio of the multiplet lines. A better fit to the experiment can be obtained by broadening the multiplets of the M_4 line group with a Fano line shape of larger width due to the shorter lifetime of these states and by adjusting the correct distance between the M_5 and the M_4 line groups by a factor of about 99%.[29]

No significant variation of the Dy $M_{4,5}$ XAS spectral line shape of the three samples is found in the temperature range from 4 to 300 K.

No variation of the line shape of Dy XAS spectra of mono- and di-*incar*-fullerenes is also found.

B. X-ray Magnetic Circular Dichroism. The element-specific magnetic orbital and spin moment of the lanthanide 4f electrons are estimated by Dy $M_{4,5}$-edge XMCD measurements providing information on the ground-state expectation value of the *z*-component of the orbital operator acting on the 4f shell that receives the photoelectron in the final state.[30] If the interaction with the cage could be neglected, the Dy ion inside the carbon cage would be prototypical of an isolated lanthanide ion with a saturation magnetization of 10 μ_B for a $4f^9$ ground-state configuration.[31] On the basis of an atomic model, the expected values of the spin $\langle S_z \rangle$ and orbital $\langle L_z \rangle$ angular momentum for free Dy^{3+} calculated by Teramura et al.[32] were $\langle L_z \rangle = -5.083\ \mu_B$ and $\langle S_z \rangle = -2.417\ \mu_B$, and the expected value for the magnetic-dipole operator $\langle T_z \rangle$ was 0.128 μ_B.

At 4 K, a strong dichroism is observed in the Dy $M_{4,5}$-edge XMCD spectra of all the investigated *incar*-fullerenes. The dichroism of different samples is first compared considering a normalized dichroic signal, calculated as $\sigma_{XMCD} = [(\sigma^+ - \sigma^-)/\max(\sigma^+ + \sigma^-)]/\delta$, where $\delta = 0.81$ is the degree of circular polarization and σ^+ and σ^- are XAS spectra obtained with right and left circular polarization, respectively, or for a fixed polarization and opposite sign of the applied magnetic field. Under a field of 7 T, at 4 K the dichroism line shape and magnitude of the two $Dy_2@C_{88}$ isomers are nearly identical for isomer I and isomer II. Therefore the symmetry of the carbon cage does not influence remarkably the *incar*-fullerene valence and magnetic moment. The dichroic signal of the Dy *incar*-fullerene in the same experimental conditions (7 T, 4 K) is about 15% *smaller* than the dichroic signal from the Dy_2 *incar*-fullerenes (Figure 2).

A quantitative estimation of the ground-state expectation values of the orbital and spin magnetic moment of the Dy 4f electrons is obtained from the XMCD experiments by the application of the magnetooptical sum rules,[30] using the ground state of the Dy ion obtained from the multiplet calculations as input information.

In the case of the Dy $M_{4,5}$-edge, $c = 2$ (3p) and $l = 3$ (4f). In the equations we have replaced the σ_0 with $(\sigma^+ + \sigma^-)/2$. The 4f shell-selective measure of the ground-state expected value of the orbital angular momentum operator L_z is

$$m_{orb}(Dy) = \langle L_z \rangle = 2\frac{\int_{L_3+L_2}(\sigma^+ - \sigma^-)\,d\omega}{\int_{L_3+L_2}(\sigma^+ + \sigma^-)\,d\omega}(14 - n_{4f})$$

$$m_{spin}(Dy) = 2\langle S_z \rangle = \frac{5\int_{L_3}(\sigma^+ - \sigma^-)\,d\omega - 3\int_{L_3+L_2}(\sigma^+ - \sigma^-)\,d\omega}{\int_{L_3+L_2}(\sigma^+ + \sigma^-)\,d\omega}(14 - n_{4f}) - 6\langle T_z \rangle$$

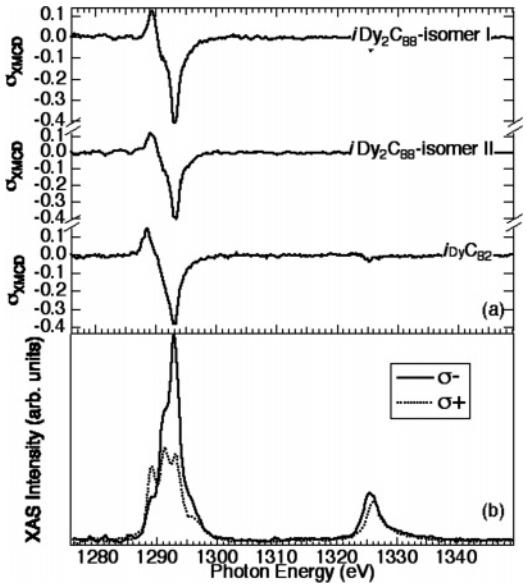

Figure 2. (a) Comparison of the σ_{XMCD} signal obtained at 7 T and 4 K for the three samples. (b) XAS spectra obtained by reversing the magnetic field using circular polarization in a field of 7 T at 4 K from $Dy_2@C_{88}$ isomer II.

where m_{orb} and m_{spin} are the orbital and spin magnetic moments expressed in units of μ_B/ion and n_{4f} is the 4f electron occupancy. The dichroic signal has been corrected for the degree of circular polarization.

For the effective occupancy of the 4f shell, we have taken $n_{4f} = 9$, considering the agreement of the experimental XAS spectra with the calculation for a $4f^9$ ground state.

The applicability of the XMCD spin sum rule has been long debated. In the $M_{4,5}$-edges of less-than-half-filled 4f shells of 4f lanthanides, the 3d−4f exchange interaction causes considerable mixing in the final state.[33] For the more-than-half-filled lanthanides, the mixing is partly suppressed and the applicability of the spin sum rule depends on the 4f electron distribution in the initial state as well as the relative strength between the 3d spin−orbit splitting and the 3d−4f exchange interaction. For the case of the 3d → 4f absorption of Dy, the deviation from the spin sum rule has been numerically calculated to be less than 10%.[32]

The $M_{4,5}$ absorption edges of lanthanides are characterized by an almost pure LSJ coupling Hund's rule ground state (L and S being angular and spin quantum numbers and J = L + S). The magnetic-dipole operator $\langle T_z \rangle$ arises from the anisotropy of the atomic charge distribution and cannot be determined from these measurements, but it can be evaluated analytically. For Dy^{3+}, calculations indicate $\langle T_z \rangle = 0.128\ \mu_B$, which is 5% of $\langle S_z \rangle$. This value was taken for $\langle T_z \rangle$ in our evaluation of the expectation value of the 4f spin moment for Dy *incar*-fullerene, but this assumption can introduce an error of about 10% in the evaluation of $\langle S_z \rangle$, if the $\langle T_z \rangle/\langle S_z \rangle$ ratio in the Dy *incar*-fullerene is the same.

Hysteresis cycles have been performed, and the presence of ferromagnetic coupling has been investigated. In the Dy *incar*-fullerene, at 4 K, a significant dichroism is visible for fields down to 0.3 T, while for the Dy_2 *incar*-fullerenes, dichroism is present down to 0.1 T (at 4 K). In both cases, Dy displays a paramagnetic behavior, with no remanence magnetization at zero field down to 4 K in agreement to what was found in ref 21 at 6 K. The ground-state expectation values of the orbital and spin magnetic moment projected on the propagation direction of the

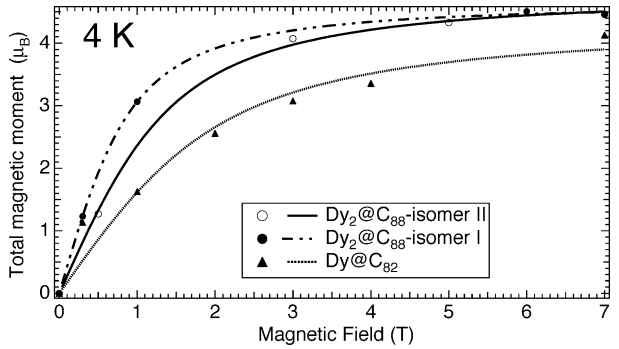

Figure 3. Field dependence of the Dy moments projected along the direction of the applied magnetic field at $T = 4$ K (markers) together with the result of the fitting using the $M(H)$ function described in the text (lines).

TABLE 1: Orbital and Spin Magnetic Moments Extracted from XMCD Data at the Indicated Temperatures and Magnetic Fields for the Measured Endohedrals and the Expected Values for a Dy^{3+} Ion

system	H (T)	T (K)	$\langle L_z \rangle$ (μ_B/ion)	$2\langle S_z \rangle$ (μ_B/ion)	$\langle M_z \rangle$ (μ_B/ion)	% reduction of L_z	% reduction of S_z	% reduction of M_z
Dy@C$_{82}$	7	4	−1.93	−2.23	4.16	62%	54%	58%
Dy@C$_{82}$	7	300	−0.322	−1.43	1.75			
Dy$_2$@C$_{88}$ isomer I	7	4	−2.32	−2.13	4.45	54%	56%	55%
Dy$_2$@C$_{88}$ isomer II	7	4	−2.20	−2.26	4.46	57%	53%	55%
Dy^{3+} (ref 32)			−5.083	−4.834	9.917			

X-rays are calculated from the experimental spectra at different applied fields and sample temperatures. The results are reported in Table 1.

At 6.9 T and 4K the two Dy$_2$@C$_{88}$ have similar orbital magnetic moments ($m_{orb} = -2.32\ \mu_B$/ion for isomer I, $m_{orb} = -2.20\ \mu_B$/ion for isomer II), while the orbital magnetic moment of Dy@C$_{82}$ is ∼12−17% smaller in the same experimental conditions. For Dy@C$_{82}$, at 6.9 T and at 4 K we have found $m_{orb} = -1.93\ \mu_B$/ion and $m_{spin} = -2.23\ \mu_B$/ion, giving a total magnetic moment of $m_{tot} = 4.16\ \mu_B$/ion. The value for the orbital magnetic moment is smaller than the one found in ref 21 ($m_{orb} = -2.73\ \mu_B$/ion), while the spin magnetic moment is comparable. At 300 K we have found $m_{orb} = -0.32\ \mu_B$/ion and $m_{spin} = -1.43\ \mu_B$/ion, giving a total magnetic moment of $m_{tot} = 1.75\ \mu_B$/ion in hartree atomic units.

The spin magnetic moment for the three samples is comparable.

In Figure 3 the total magnetic moment of the three samples calculated from the application of the sum rules to the XMCD spectra measured as a function of the applied field at $T = 4$ K is shown.

For all compounds, the magnetic moment of 4f orbitals increases with the applied magnetic field, due to the progressive alignment of the magnetic moments of the 4f orbitals. For each sample the field dependence of the Dy moment has been fitted with the function $M(H) = ngJ\mu_B B_J(x)$, where n was a fitting parameter, $g = {}^3/_2 + ({}^1/_2)\{[S(S+1) - L(L+1)]/[(L+S)(L+S+1)]\}$, $L = 5$, $S = {}^5/_2$, $J = {}^{15}/_2$, and $B_J(x)$ was the Brillouin function with $x = g\mu_B H/(k_B T)$.[12] At 4 K the samples are not fully saturated in a magnetic field of 7 T, and the magnetic moment is from 2% to 5% less than the saturation value extracted from the fit of the field dependence of the total magnetic moment.

For Dy@C$_{82}$ the local magnetic moment of the 4f orbitals grows more slowly than those for the two Dy$_2$@C$_{88}$ isomers.

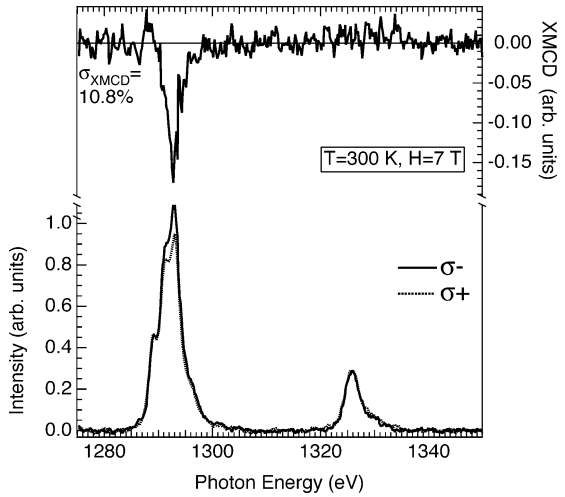

Figure 4. Dy $M_{4,5}$-edge XMCD spectrum of Dy@C$_{82}$ at 300 K and 7 T.

For Dy@C$_{82}$, a small but significant dichroism has been detected at 300 K from 7 to 4 T (Figure 4).

No significant circular dichroism (below 1%) was detected in the XMCD spectra measured across C K edge recorded at 4 K under fields of 4 and 7 T either by reversing the magnetic field or by reversing the polarization, indicating that C atoms do not carry significant magnetic moments.[34]

Calculations of the σ^+ and σ^- XAS spectra and their difference (the XMCD spectra) also have been performed, and they are reported in Figure 7. The calculation of the XMCD line shape has been performed using the method described in ref 28. The intensity distribution of the optical dipole transitions has been multiplied by the square of the 3*j*-symbol according to the Wigner−Eckart theorem, considering a Boltzmann population distribution and the polarization vector perpendicular to the magnetic field ($\Delta M \pm 1$).

C. Resonant Photoemission. We performed valence band 3d → 4f RESPES measurements of Dy$_2$@C$_{88}$, selecting the excitation energy on-resonance at the position of the various multiplet structures I−IV observed in the Dy M_5-edge XAS spectrum in Figure 1 and off-resonance at $h\nu = 1249$ eV (OFF). Through the use of photon energies close to the 3d → 4f threshold, the Dy spectral weight in the valence band is resonantly enhanced (Figure 5a). The components extracted from the fitting procedure are labeled A (4.0 eV), B (7.0 eV), C (10.0 eV), D (15.5 eV), and E (25.5 eV) (Figure 5b). In Figure 6 we report the difference spectra obtained by subtracting the spectra off-resonance from each on-resonance spectrum. From the difference spectra and from the peak intensity extracted from the fitting procedure peaks B and C appear enhanced on-resonance. By comparing the difference spectra and the valence band of metallic dysprosium[35] and multiplet calculations[36] we can ascribe component C to Dy 4f quintuplet states. Component B is partly coming from the septet ^{7}F Dy 4f states and partly from Au $5d_{3/2}$ of the substrate. Component A mainly arises from Au $5d_{5/2}$ emission. Peak E is due to Dy 5p emission. Dy binding energies in Dy$_2$@C$_{88}$ are shifted by 2.5−3 eV to higher values with respect to the metallic Dy.

IV. Discussion

The magnetic moment of the Dy ions inside the carbon cage derived from XMCD is significantly smaller (55−60%) than the magnetic moment of the free Dy^{3+} ion. The entity of the orbital magnetic moment reduction is lower in the di-*incar*-

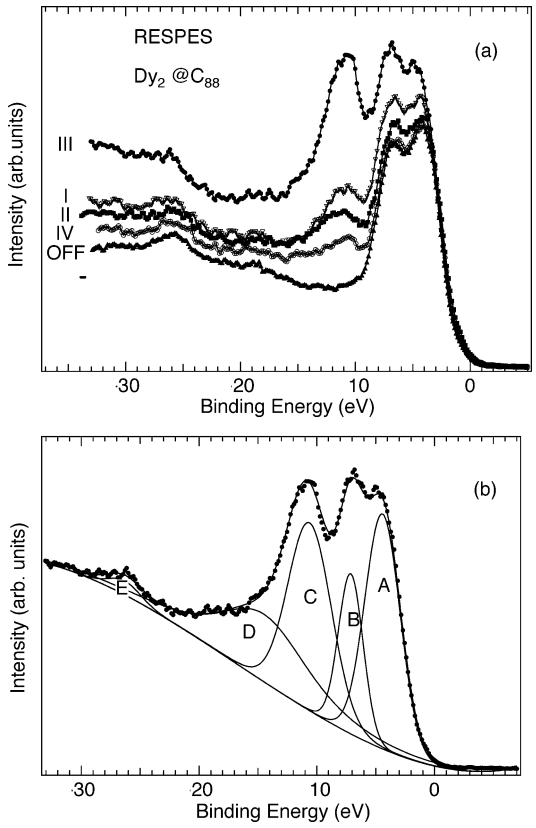

Figure 5. Photoemission spectra acquired at photon energies I−IV (Figure 1).

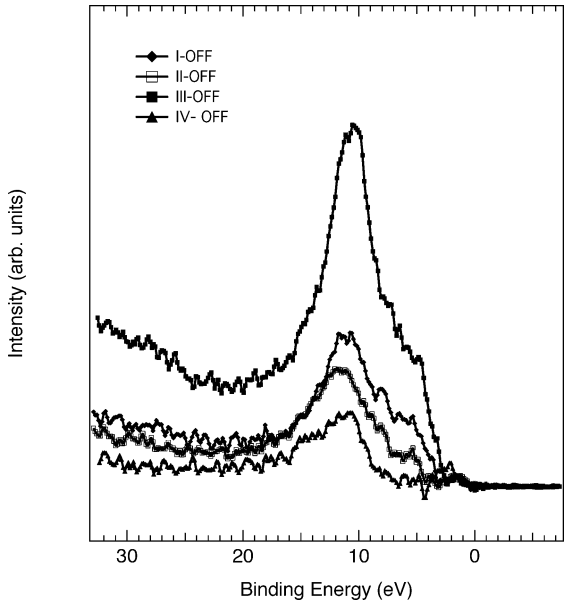

Figure 6. Spectra obtained after subtraction the off-resonance PES spectrum from the spectra acquired at photon energies I−IV.

fullerenes with respect to the mono-*incar*-fullerene, whereas the spin magnetic moments are similar. Noteworthy, the reduction of the magnetic moment we observe in XMCD at 4 K and 7 T (50−60%) is much higher than that obtained from SQUID measurements (∼20%).[12] From the application of the sum rules to the measured spectra we have observed there is not only quenching of the orbital moment since both m_{orb} and m_{spin} are reduced by about 50% with respect to the values expected for Dy^{3+}. In section III.B we have discussed the applicability of sum rules for the quantitative estimation of the Dy magnetic

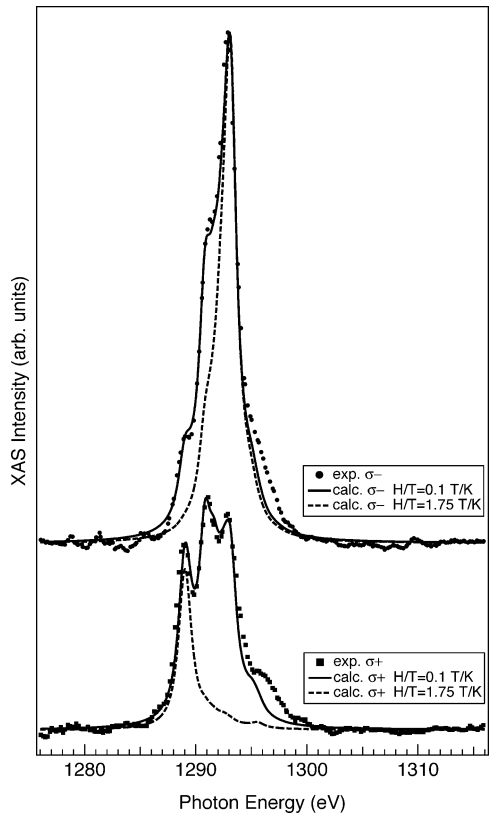

Figure 7. Dy $M_{4,5}$-edge XAS experimental spectrum of the $Dy_2@C_{88}$ isomer II measured at 4 K with a magnetic field of 7 T using right (σ^+) and left (σ^-) polarization and the results of atomic calculations performed with the same atomic parameters used for the calculations of Figure 1 for $H/T = 1.75$ T/K and $H/T = 0.1$ T/K (assuming 100% polarization rate).

moment from Dy $M_{4,5}$ XMCD and the possible complications due to *jj*-mixing or a wrong estimation of the T_z value. These factors should not play a major role for Dy due to its more-than-half-filled 4f shell. The validity of sum rules can also be affected by saturation effects, which, in total-electron-yield XAS signal, are known to be significant for lanthanides over the range of soft X-ray energy.[29] However we found a good reproducibility of the calculations with the experimental XAS spectrum and we also found a correct L_z/S_z ratio as expected for expected for the Dy^{3+} Hund's rule state, so no major problems of signal saturation affect the data. In the following we examine other possible explanations for the observed XMCD reduction of the magnetic moment of Dy *incar*-fullerenes.

First we consider a possible underestimation of the magnetic moment due to the low temperature (4 K) at which the magnetic moment has been evaluated. Isothermal SQUID magnetization measurements indicate that the effective magnetic moment levels off to a maximum value around 75 K, and the effective magnetic moment for $Dy@C_{82}$ is estimated to be around 5−5.5 μ_B at 4 K.[12] For high fields and low temperatures, SQUID data found deviations of the magnetization from the Curie−Weiss law and the expected linear M−H relationship.[12] These deviations have been associated with magnetic interactions between core atoms and carbon cage crystal field splitting that become more pronounced at low temperatures maybe due to an orientation ordering transition.

We then consider the possibility that the reduction of the magnetic moment derived from XMCD relative to that found from SQUID can be also due to the presence of 5d Dy states. In Er solid calculations indicate that the 5d6s electrons contribu-

tion to the magnetic moment is about 10%.[37] If 5d orbitals are present, then they would contribute to the magnetic moment, but their contribution would not be detected by Dy $M_{4,5}$-edge XMCD, which is essentially sensitive to the magnetic moment of the Dy 4f orbitals. The presence of spectral weight from 5d electrons in the valence band has been therefore investigated by 3d → 4f RESPES measurements. In Dy metal and in some Dy compounds such as DyTe, at E_F a band, ascribed to a 5d band and shifted by about 3−4 eV from the lowest-energy 4f structure, is strongly enhanced at resonance. In the difference spectra obtained from the spectrum measured on-resonance and the spectrum measured off-resonance, no significant enhancement of spectral intensity is observed in $Dy_2@C_{88}$ where Dy 5d states are expected. The lack of significant density of states close to the Fermi level is in agreement with a previous Mössbauer study of the same system, which indicates a full charge transfer from Dy to the carbon cage and therefore no electrons in 5d orbitals.[15]

We then consider the effect of the substrate. Since the film was not homogeneous, layers of different thickness were probed at the same time. The measured spectra thus can carry the contribution of sub-monolayers, where the effect of the substrate can be important. We expect that charge transfer from the substrate to the carbon cage and crystal field would have the effect to decrease the Dy magnetic moment in sub-monolayers. This would also explain the slightly larger orbital magnetic moment obtained in ref 21 from homogeneous $Dy@C_{82}$ thick films in similar experimental conditions and the larger moment obtained by SQUID.

An incomplete saturation of the system is another possible reason for the reduction of the magnetic moment relative to the free ion. From the fit of the magnetization curve versus the applied field, the saturation value is only 2−5% higher, while calculations of the σ^+ and σ^- XAS spectra assuming $T = 4$ K and $H = 7$ T and a spherical environment do not match with the experimental spectra. In particular, in the calculated σ^+ spectrum only the $\Delta J = +1$ component is present, while for the calculated σ^- spectrum only the $\Delta J = -1$ component is present. The $\Delta J = 0$ component visible in the experimental data is very small in the calculations. The $\Delta J = 0$ component increases, and the agreement between calculated and experimental RCP-LCP (Right Circular Polarization−Left Circular Polarization) components becomes very good if H/T is taken to be 0.10 T/K for 100% polarization rate and 0.12 T/K for 81% polarization rate (Figure 7). This would be explained if a fraction of the Dy atoms have a magnetization directed along a different direction from that of the applied field. Considering that XMCD gives the average Dy moment projected along the magnetic field, this result may indicate a noncollinear arrangement of the magnetic moments due to the large local anisotropy originated by the large spin−orbit coupling.[38]

Finally we consider the reduced symmetry of the Dy ion due to its off-center position inside the cage. In endohedrals large electric dipole moments are expected, giving rise to the uniaxial orientation of the molecules. At low temperatures a quenching of the molecular rotation occurs, and the motion of the encapsulated atom inside the cage, which is present at room temperature,[19] is expected to be also reduced. Furthermore, in $Ce@C_{82}$, the field cooling effect on the susceptibility indicates that the application of a magnetic field forces the molecular orientation to be aligned.[39] These effects would induce a large low-symmetry crystal field, which, together with the large orbital moment, would induce magnetic anisotropy. Due to the off-centered position of the Dy encaged in C_{82},[20,40] the metal can experience a crystal field similar to that present at the interface between a substrate and adsorbed layers of lanthanide atoms. Dy epitaxial layers, for example, exhibit strong linear dichroism due to the presence of a crystal field that modifies the relative weights of the ΔJ transitions.[41] A magnetic moment reduction relative to free ion values was also observed in lanthanide carbides. This reduction was explained by the crystal field splitting of the lanthanide ion ground-state energy level.

Similarly, the difference in the orbital moment of $Dy_2@C_{88}$ and $Dy@C_{82}$ (while the spin magnetic moment is nearly the same) would be explained by a different crystal field acting on the Dy ions due to a different coordination.

V. Conclusions

The local electronic and magnetic properties of *incar*-fullerenes $Dy@C_{82}$ and $Dy_2@C_{88}$ have been investigated by X-ray core-level spectroscopic techniques at resonance conditions.

Both the single encaged Dy and the encaged Dy pair are found in a $4f^9$ configuration. The measurements indicate a full charge transfer from Dy to the fullerene cage. Isothermal magnetization loops at 4 K indicate that the magnetic moment is not fully saturated at 7 T. Dy displays a paramagnetic behavior, with no remaining magnetization at zero field down to 4 K. A significant magnetic moment is detected at 300 K and 6.9 T. The ground-state expected values of the orbital and spin magnetic moment projected on the propagation direction of the X-rays are calculated from the experimental spectra at different applied fields and sample temperatures. At 6.9 T and 4 K the two di-*incar*-fullerenes have similar orbital magnetism, while the orbital magnetic moment of the mono-*incar*-fullerene is ∼15% smaller in the same experimental conditions. The 4f local moments grow faster for the di-*incar*-fullerenes than that for the mono-*incar*-fullerene as a function of the applied field. The di-*incar*-fullerenes and the mono-*incar*-fullerene have similar spin magnetic moments, while the orbital magnetic moment is larger for $Dy_2@C_{88}$. Both the orbital and the spin magnetic moments of the Dy atoms inside the carbon cage at 6.9 T and 4 K are dramatically smaller than those expected for the free Dy^{3+} at saturation. Incomplete saturation, substrate, and symmetry reduction effects are discussed as possible factors contributing to the reduction of the magnetic moment.

Acknowledgment. The authors thank Frank de Groot for supplying us with his computer program package and useful advice in the calculation of the XMCD spectra. We gratefully thank Jean Paul Kappler for the installation and the assistance with the CNRS cryostat as well for fruitful discussion and Stefania Pagliara for stimulating discussions. Finally we thank Petra Rudolf for providing us with their data prior to publication and for several discussions. N.T. gratefully acknowledges financial support by the European Heads of Research Councils in collaboration with the European Science Foundation through the European Young Investigator (EURYI-2004) Awards Scheme.

References and Notes

(1) Shinohara, H. *Rep. Prog. Phys.* **2000**, *63*, 843.
(2) Lu, X.; Xu, J. X.; Shi, Z. J.; Sun, B. Y.; Gu, Z. N.; Liu, H. D.; Han, H. B. *Chem. J. Chin. Univ.* **2004**, *25*, 697.
(3) Kato, H.; Kanazawa, Y.; Okumura, M.; Taninaka, A.; Yokawa, T.; Shinohara, H. *J. Am Chem. Soc.* **2003**, *125*, 4391.
(4) Shinohara, H.; Yagi, K.; Nakamura, K. Japanese Patent 143,478, 1996.
(5) Mikawa, M.; Kato, H.; Okumura, M.; Narazaki, M.; Shinohara, H. *Bioconjugate Chem.* **2001**, *12*, 510.
(6) Cagle, D. W.; Alford, J. M.; Tien, J.; Wilson, J. In *Fullerenes: Recent Advances in the Chemistry and Physics of Fullerenes and Related*

Materials; Kadish, K. M., Ruoff, R. S., Eds.; The Electrochemical Society: Pennington, NJ, 1995; Vol. 2, p 361.

(7) Wilson, L. J.; Cagle, D. W.; Thrash, T.; Kennel, S. J.; Mirzadeh, S.; Alford, J. M.; Ehrhardt, G. J. *Coord. Chem. Rev.* **1999**, *190*−*192*, 199.

(8) Yang, S.; Fan, L.; Yang, S. *J. Phys. Chem. B* 2004, *108*, 4394.

(9) Slanina, Z.; Kobayashi, K.; Nagase, S**.** Computing Metallofullerenes as Agents of Nanoscience: Gibbs Energy Treatment of Ca@C_{72}, Ca@C_{82}, and La@C_{82}. In *Nanotech 2004*, Technical Proceedings of the 2004 NSTI Nanotechnology Conference and Trade Show; Laudon, M., Romanowicz, B., Eds.; Computational Publications: Cambridge, MA, 2004; Vol. 3.

(10) Kessler, B. Bringer, A.; Cramm, S.; Schlebusch, C.; Eberhardt, W. Suzuki, S.; Achiba, Y. Esch, F.; Barnaba, M.; Cocco, D. *Phys. Rev. Lett.* **1997**, *79*, 2289.

(11) Pichler, T.; Hu, Z.; Grazioli, C.; Legner, S.; Knupfer, M.; Golden, M. S.; Fink, J.; de Groot, F. M. F.; Hunt, M. R. C.; Rudolf, P.; Follath, R.; Jung, Ch.; Kjeldgaard, L.; Brühwiler, P. A.; Inakuma, M.; Shinohara, H. *Phys. Rev. B* **2000**, *62*, 13196.

(12) Huang, H. J.; Yang, S. H.; Zhang, X. X. *J. Phys. Chem. B* **2000**, *104*, 1473.

(13) Pagliara, S.; Sangaletti, L.; Cepek, C.; Bondino, F.; Larciprete, R.; Goldoni, A. *Phys. Rev. B* **2004**, *70*, 035420.

(14) Funasaka, H.; Sugiyama, K.; Yamamoto, K.; Takahashi, T. *J. Phys. Chem.* **1995**, *99*, 1826.

(15) Grushko, Y. S.; Alekseev, E. G.; Kozlov, V. S.; Molkanov, L. I.; Wortmann, G.; Giefers, H.; Rupprecht, K.; Khodorkovskii, M. A. *Hyperfine Interact.* **2000**, *126*, 121.

(16) Johansson, B. *Phys. Rev. B* **1979**, *19*, 6615.

(17) Patthey, F.; Bullock, E. L.; Schneider, W.-D.; Hulliger, F. *Z. Phys. B* **1993**, *93*, 71.

(18) Iida S, S.; Kubozono, Y.; Slovokhotov, Y.; Takabayashi, Y.; Kanbara, T.; Fukunaga, T.; Fujiki, S.; Emura, S.; Kashino, S. *Chem. Phys. Lett.* **2001**, *338*, 21.

(19) Kubozono, Y.; Takabayashi, Y.; Shibata, K.; Kanbara, T.; Fujiki, S.; Kashino, S.; Fujiwara, A.; Emura, S. *Phys. Rev. B* **2003**, *67*, 115410.

(20) Wang, K.; Zhao, J.; Yang, S.; Chen, L.; Li, Q.; Wang, B.; Yang, S.; Yang, J.; Hou, J. G.; Zhu, Q. *Phys. Rev. Lett.* **2001**, *91*, 185504.

(21) De Nadaï, C.; Mirone, A.; Dhesi, S. S.; Bencok, P.; Brookes, N. B.; Marenne, I.; Rudolf, P.; Tagmatarchis, N.; Shinohara, H.; Dennis, T. J. S. *Phys. Rev. B* **2004**, *69*, 184421.

(22) Zangrando, M.; Zacchigna, M.; Finazzi, M.; Cocco, D.; Rochow, R.; Parmigiani, F. *Rev. Sci. Instrum.* **2004**, *75*, 31.

(23) Tagmatarchis, N.; Shinohara, H. *Chem. Mater.* **2000**, *12*, 3222.

(24) Tagmatarchis, N.; Aslanis, E.; Prassides, K.; Shinohara, H. *Chem. Mater.* **2001**, *13*, 2374.

(25) (a) Sainctavit, Ph.; Lefebvre, D.; Cartier, Ch.; Laffon, C.; Krill, G.; Brouder, Ch.; Kappler, J.-P.; Schillé, J.-Ph.; Goulon, J. *J. Appl. Phys.* **1992**, *72*, 1985. (b) Sainctavit, Ph.; Lefebvre, D.; Arrio, M.-A.; Cartier dit Moulin, Ch.; Kappler, J.-P.; Schillé, J.-Ph.; Krill, G.; Brouder, Ch.; Verdaguer, M. *Jpn. J. Appl. Phys.* **1993**, *32*, 295.

(26) Cowan, R. *The Theory of Atomic Structure and Spectra*; University of California Press: Berkeley, CA, 1981.

(27) de Groot, F. M. F.; Vogel, J. Fundamentals of X-ray Absorption and Dichroism: The Multiplet Approach; In *Neutron and X-ray Spectroscopy*; Hippert, F., Geissler, E., Hodeau, J.-L., Leliévre−Berna, E., Regnard, J.-R., Eds.; Springer: New York, 2006.

(28) Goedkoop, J. B.; Thole, B. T.; van der Laan, G.; Sawatzky, G.; de Groot, F. M. F.; Fuggle, J. C. *Phys. Rev. B* **1988**, *37*, 2086.

(29) Thole, B. T.; van der Laan, G.; Fuggle, J. C.; Sawatzky, G. A.; Karnatak, R. C.; Esteva, J.-M. *Phys. Rev. B* **1985**, *32*, 5107.

(30) (a) Thole, B. T.; Carra, P.; Sette, F.; van der Laan, G. *Phys. Rev. Lett.* **1992**, *68*, 1943. (b) Carra, P.; Thole, B. T.; Altarelli, M.; Wang, X. *Phys. Rev. Lett.* **1993**, *69*, 2307.

(31) Ashcroft, N. W.; Mermin, N. D. *Solid State Physics*; Saunders College Publishing: New York, 1976.

(32) Teramura, Y.; Tanaka, A.; Thole, B. T.; Jo, T. *J. Phys. Soc. Jpn.* **1996**, *65*, 3056.

(33) Jo, T. *J. Phys. Soc. Jpn.* **1997**, *86*, 73

(34) Bondino, F.; Cepek, C.; Goldoni, A. Unpublished work.

(35) Arenholz, E.; Navas, E.; Starke, K.; Baumgarten, L.; Kaindl, G. *Phys. Rev. B* **1995**, *51*, 82111.

(36) Gerken, F. *J. Phys. F: Met. Phys.* **1983**, *13*, 703.

(37) Huang, Z.; Ye, L.; Yang, Z. Q.; Xie, X. *Phys. Rev. B* **2000**, *61*, 12786.

(38) Garcia, L. M.; Pizzini, S.; Rueff, J. P.; Vogel, J.; R. M. Galéra, Fontaine, A.; Kappler, J. P.; Krill, G.; Goedkoop, J. *J. Appl. Phys.* **1996**, *79*, 6497.

(39) Inakuma, M.; Kato, H.; Taninaka, A.; Shinoara, H.; Enoki, T. *J. Phys. Chem. B* **2003**, *107*, 6965.

(40) Iida, S.; Kubozono, Y.; Slovokhotov, Y.; Takabayashi, Y.; Kanbara, T.; Fukunaga, T.; Fujiki, S.; Emura, S.; Kashino, S. *Chem. Phys. Lett.* **2001**, *338*, 21.

(41) (a) Vogel, J.; Sacchi, M.; Sirotti, F.; Rossi, G. *Appl. Surf. Sci.* **1993**, *65*, 170. (b) Sacchi, M.; Sakho, O.; Sirotti, F.; Rossi, G. *Appl. Surf. Sci.* **1992**, *56*, 1.